Supporting Information

Efficient inverse CO_2/C_2H_2 separation driven by rare thermodynamic affinities difference in a porous MOF

Hai-Yu Duan[a], Xiu-Yuan Li*[a], Lei Hou*[b], Si-Ru Liu[a], Xiang-Yu Liu*[c], Ping Wang*[a]

[a]Shaanxi Key Laboratory of Optoelectronic Functional Materials and Devices, School of Materials Science and Chemical Engineering, Xi'an Technological University, Xi'an, 710021, P. R. China. E-mail: lixiuyuan@xatu.edu.cn, wping0922@163.com

[b]Key Laboratory of Synthetic and Natural Functional Molecule Chemistry of the Ministry of Education, Shaanxi Key Laboratory of Physico-Inorganic Chemistry, College of Chemistry & Materials Science, Northwest University, Xi'an 710069, P. R. China. E-mail: lhou2009@nwu.edu.cn

[c]State Key Laboratory of High-efficiency Coal Utilization and Green Chemical Engineering, College of Chemistry and Chemical Engineering, Ningxia University, Yinchuan 750021, P. R. China. E-mail: xiangyuliu432@126.com

Table S1 Summary of adsorption uptakes, Q_{st} values and selectivity of equimolar CO_2/C_2H_2 mixture for reported CO_2-selective MOFs.

MOFs	Uptake of CO_2/C_2H_2 @273K, 100 kPa ($cm^3\ g^{-1}$)	Uptake of CO_2/C_2H_2 @298K, 100 kPa ($cm^3\ g^{-1}$)	Q_{st} of CO_2/C_2H_2 (kJ mol^{-1})	Selectivity	Selectivity Conditions	*Ref.*
[Co(HL[dc])]	108/-	239.5[e]/140[e]	\	\	\	1
[Mn(bdc)(dpe)]	46.8[a]/7.3[a]	\	29–30/28	8.8	273 K, 100 kPa	2
SIFSIX-3-Ni	\	2.7[c]/3.3[c]	50.9/36.7	7.7[j]	298 K, 1 bar	3
CD-MOF-1	\	2.87[c]/2.23[c]	41.0/17.6	6.6[j]	298 K, 100 kPa	4
CD-MOF-2	\	2.67[c]/2.03[c]	67.2/25.8	16.0[j]	298 K, 100 kPa	4
Tm-MOF	146.3/63.0	130.6/47	45.2/17.8	17.5[j]	298 K, 1 bar	5
MUF-16	\	47.78[f]/3.99[f]	32.3/-	510	293 K, 1 bar	6
MUF-16(Ni)	\	47.97[f]/7.53[f]	37.3/-	46	293 K, 1 bar	6
MUF-16(Mn)	\	50.5[f]/9.69[f]	36.6/-	31	293 K, 1 bar	6
Cd-NP	\	58.0/9.7	27.7/-	85	298 K, 1 bar	7
PCP-NH_2-ipa	\	72/43	36.6/26.8	6.4	298 K, 1 bar	8
PCP-NH_2-bdc	\	68/43	34.57/25.6	4.4	298 K, 1 bar	8

Ce(IV)-MIL-140-4F	151.7[b]/53.5[b]	110.3[b]/41.5[b]	39.5/27.4	9.5[j]	298 K, 100 kPa	9
PMOF-1	47.5/9.5	\	\	\	\	10
[Zn(atz)(BDC-Cl_4)$_{0.5}$]$_n$	60.2[b]/-	19.7[b]/-	32.7/25.4	2.4	285 K, 100 kPa	11
Cu-F-pymo	\	1.19[c]/0.10[c]	28.8/-	>10^5	298 K, 100 kPa	12
[Cu(hfipbb)(H_2hfipbb)$_{0.5}$]	0.75[c]/0.03[c]	0.74[c]/0.10[c]	25.5/-	696	298 K, 1 bar	13
SU-101(Bi)	\	53.7/51.4	30.5/28.8	5.5	298 K, 100kPa	14
SU-101(Al)	\	53.1/-	31.3/-	15.5	298 K, 100 kPa	14
SU-101(In)	\	55.0/-	28.3/-	6.2	298 K, 100 kPa	14
SU-101(Ga)	\	40.2/-	27.7/-	11.1	298 K, 100 kPa	14
[Zn(odip)$_{0.5}$(bpe)$_{0.5}$(CH_3OH)]	118.8/59.0	118.7/39.8	42.3/35.0	13.2	298 K, 100 kPa	15
ZU-610a	\	1.51[c]/0.12[c]	27.3/-	207	298 K, 100 kPa	16
Y-bptc	\	55/-	31.5/-	4.1	298 K, 1bar	17
SNNU-334	85.1/66.8	\	20.2/38.3	3595.4	273 K, 1atm	18
SNNU-335	78.4/63.0	\	38.07/44.23	\	\	18
SNNU-336	92.7/65.3	\	50.9/48.7	\	\	18

MOF-808-ARG (dry)	\	51.0/41.3	48.3/38.8	3.5[j]	298 K, 1 bar	19
MOF-808-ARG (wet)	\	71.0/7.8	70.3/5.2	71[j]	298 K, 1 bar	19
Bi-MOF-CHO	\	147.7[b]/81.8[b]	48.2/46.2	7.7	298 K, 100 kPa	20
Bi-MOF-COOH	\	114.7[b]/-	43.6/40.6	5.3	298 K, 100 kPa	20
Bi-MOF-NO_2	\	129.1[b]/-	38.8/38.5	4.9	298 K, 100 kPa	20
BUCT-C19	\	40.3/6.7	\	10700	298 K, 100 kPa	21
F4_MIL-140A(Ce)	\	2.6[c]/-	35-45/-	\	\	22
MFU-4	\	3.17[c, g]/-	24/-	3360	300 K, 1bar	23
Zn-DPNA	61.1/92.1	52.7/-	43.1/32.4	11.9	298 K, low pressure	24
ALF	\	86.2/3.3	\	6.5×10^5	298 K, 100 kPa	25
NKMOF-9a	57.5/4.9	46.4/2.8	69.6/-	241.9	298 K, 1 bar	26
Zn-ox-mtz	\	68.78/5.46	43.02/-	1064.9	298 K, 1.0 bar	27
Zn-ox-trz	\	89.49/67.85	38.09/38.39	1.9	298 K, 1.0 bar	27
Co-CUK-1	170[d]/119[d]	106/86	20.8/-	2	298 K, 100 kPa	28
Ni-CUK-1	142[d]/97[d]	\	21.7/-	2	298 K, 100 kPa	28

Mg-CUK-1	144[d]/89[d]	\	\	2	298 K, 100 kPa	28
HOF-FJU-88	\	59.6[h]/6.28[h]	12.3/-	1894	296 K, 1 bar	29
$Cu(Qc)_2$	\	66.6[b]/26.5[b]	31.7±3.5/ 21.4±3.5	5.6	298 K, 1 bar	30
1	74.6/45.5	57.0/37.9	38.7/29.0	3.0	298 K, 100 kPa	This work

[a] at 273 K, 91 kPa;

[b] gas uptake (cm^3 cm^{-3});

[c] gas uptake (mmol g^{-1});

the gas uptakes of CO_2 and/or C_2H_2 [d] at 233 K, [e] at 195 K, [f] at 293 K, [g] at 300 K, [h] at 296 K, [i] at 298 K and 5 bar;

[j] the mixture of CO_2/C_2H_2 (1:2, v:v).

Table S2 Structures data and selected refinement of **1**.

Complex	**1**
Molecular Formula	$C_{20}H_{19}Ca_2NO_{12}$
Formula Weight	545.52
Temperature (K)	293(2) K
Crystal System	Triclinic
Space Group	$P\bar{1}$
a (Å)	10.2890(4)
b (Å)	11.6704(6)
c (Å)	12.4006(10)
α (°)	71.553(6)
β (°)	66.005(6)
γ (°)	68.890(4)
V ($Å^3$)	1243.56(15)

Z	2
Dc (g·cm^{-3})	1.457
F(000)	564
Reflections collected	10350
Goodness-of-fit on F^2	1.049
R_1[a][$I>2\sigma(I)$]	0.0760
wR_2[b][$I>2\sigma(I)$]	0.2188

[a] $R_1 = \Sigma||F_o| - |F_c||/\Sigma|F_o|$. [b] $wR_2 = [\Sigma w(F_o^2 - F_c^2)^2/\Sigma w(F_o^2)^2]^{1/2}$

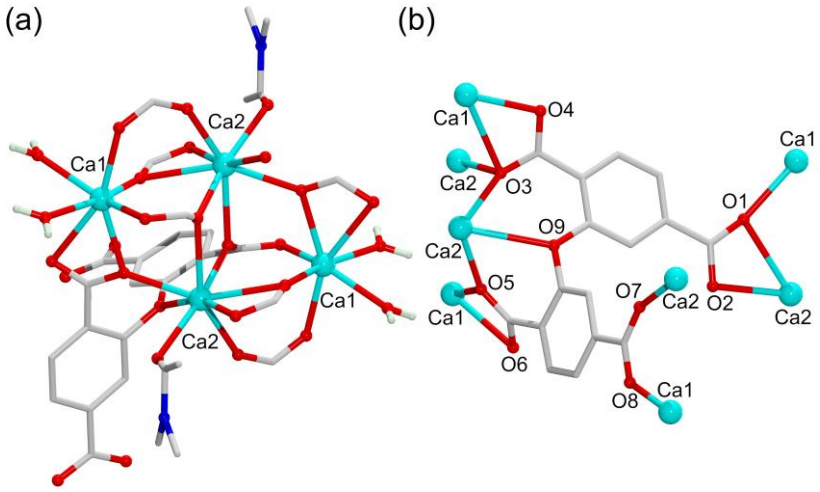

Fig. S1 (a) Coordination environment of Ca^{2+} ion; (b) Coordination mode of H_4odp.

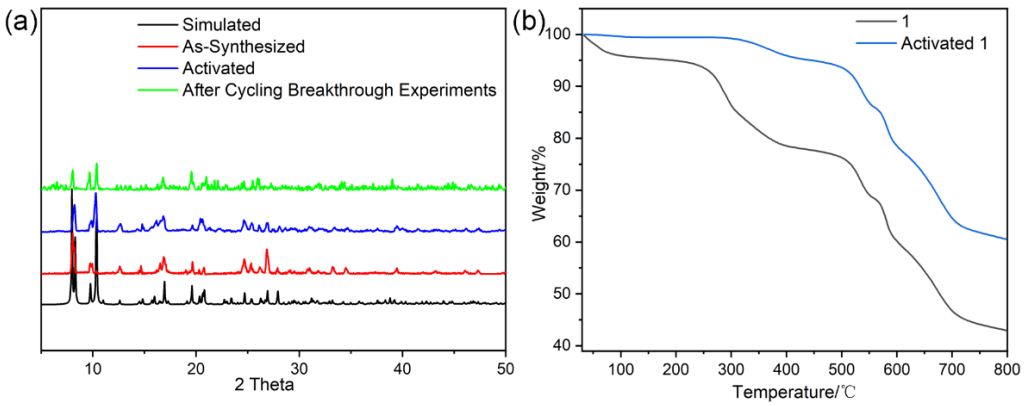

Fig. S2 PXRD and TGA patterns.

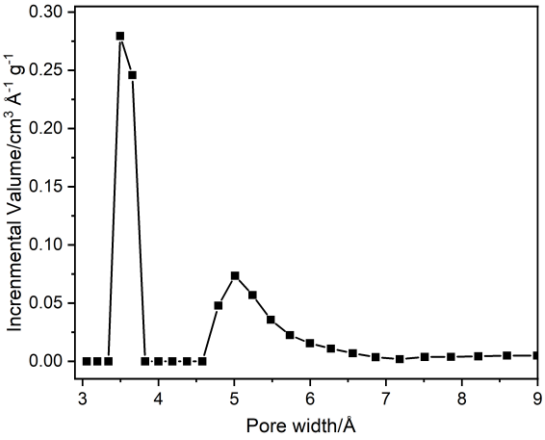

Fig. S3 The pore size distributions obtained by the non-local density-functional theory (NLDFT) model from CO_2 at 273 K.

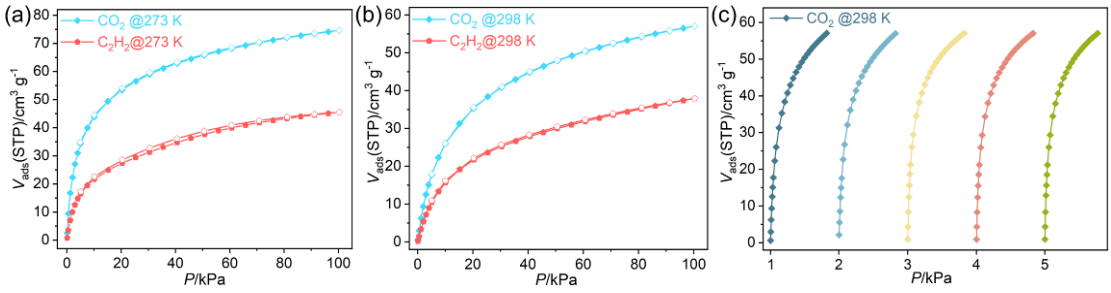

Fig. S4 Gas sorption isotherms (units: $cm^3\ g^{-1}$) for CO_2 and C_2H_2 at (a) 273 K and (b) 298 K; (c) Cyclic CO_2 sorption isotherms at 298 K.

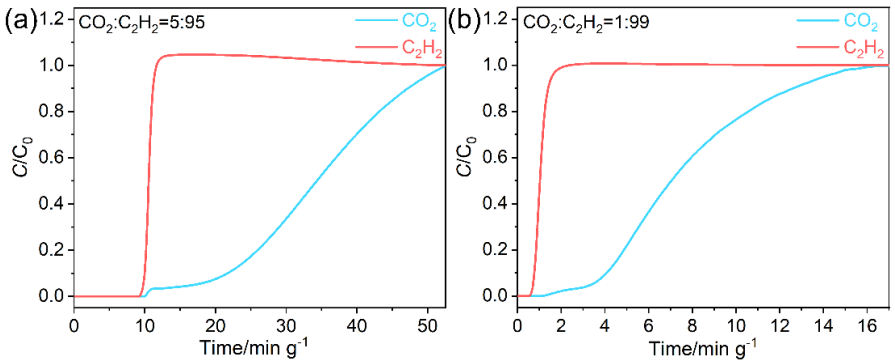

Fig. S5 Breakthrough curves for (a) 5/95 and (b) 1/99 CO_2/C_2H_2 mixtures.

Calculation of Sorption Heat using Virial 2 Model

$$\ln P = \ln N + 1/T \sum_{i=0}^{m} a_i N^i + \sum_{i=0}^{n} b_i N^i \qquad Q_{st} = -R \sum_{i=0}^{m} a_i N^i$$

The above virial expression was used to fit the combined isotherm data for three frameworks at 273 and 298 K, where *P* is the pressure, *N* is the adsorbed amount, *T* is the temperature, a_i and b_i are virial coefficients, and *m* and *N* are the number of coefficients used to describe the isotherms. Q_{st} is the coverage-dependent enthalpy of adsorption and *R* is the universal gas constant.

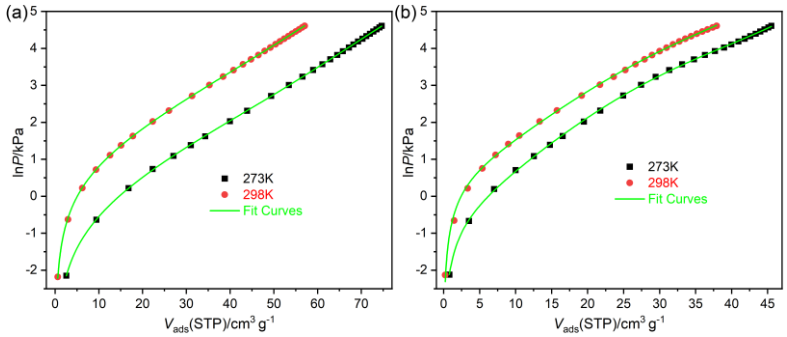

Fig. S6 (a) CO_2 and (b) C_2H_2 adsorption isotherms of **1a** with fitting by Virial 2 model.

Table S3 Parameters obtained from the Virial 2 model fitting of the single-component adsorption isotherms of CO_2 and C_2H_2 at 273 K and 298 K.

	a0	a1	a2	a3	a4	a5	b0	b1	b2	b3	Chi^2	R^2
CO_2	-4678.02	34.6279	-0.7279	-1.80E-04	9.81E-05	-5.12E-07	13.9894	-0.10383	0.00352	-2.30E-05	1.12E-04	1
C_2H_2	-3505.79	82.8451	-0.59184	-0.04199	7.24E-04	-2.06E-06	10.9831	-0.33925	0.01012	-8.08E-05	2.08E-03	0.999

CO_2/C_2H_2 Mixtures Selectivity Prediction via IAST

The experimental isotherm data for pure CO_2 and C_2H_2 were fitted using a dual Langmuir-Freundlich (L-F) model:

$$q = \frac{a_1 * b_1 * p^{c1}}{1 + b_1 * p^{c1}} + \frac{a_2 * b_2 * p^{c2}}{1 + b_2 * p^{c2}}$$

Where q and p are adsorbed amounts and the pressure of component i, respectively.

The adsorption selectivities for binary mixtures defined by

$$S_{i/j} = \frac{x_i * y_j}{x_j * y_i}$$

were respectively calculated using IAST. Where x_i is the mole fraction of component i in the adsorbed phase and y_i is the mole fraction of component i in the bulk.

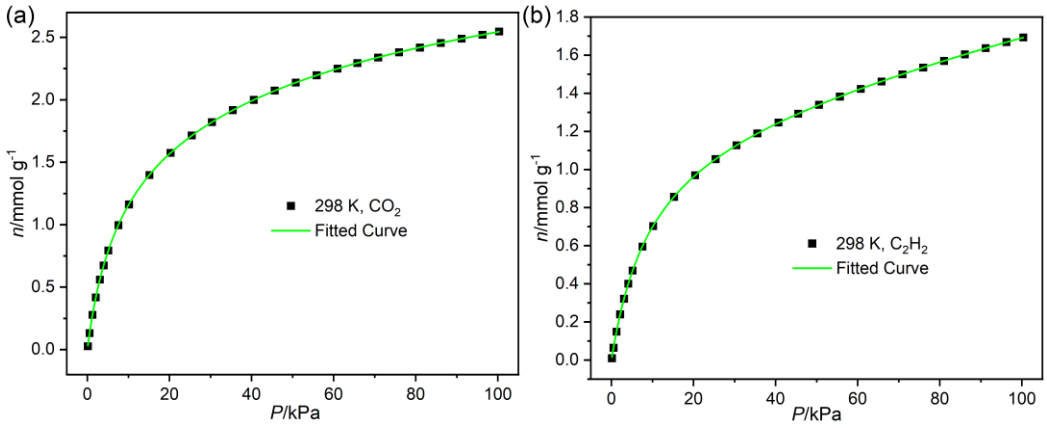

Fig. S7 Adsorption isotherms of **1a** fitting by dual L-F model.

Table S4 Parameters obtained from the dual Langmuir-Freundlich fitting of the single-component adsorption isotherms.

298 K	a1	b1	c1	a2	b2	c2	Chi^2	R^2
CO_2	1.52099	0.14252	0.99064	2.17614	0.01862	0.8798	1.99E-06	1
C_2H_2	1.18319	0.10654	1.01937	8.03444	0.00109	0.93587	2.26E-06	1

Separation Potential Calculation

The separation potential (Δq) is a combined metric, which incorporates both uptake capacity and selectivity, which is defined to evaluate the separation performances in fixed bed adsorbers for gas mixture. The separation potential Δq, is calculated from IAST base on the following equation:

$$\triangle q = q_1 \frac{y_2}{y_1} - q_2$$

Where y_1 and y_2 are the mole fractions of the CO_2 and C_2H_2 in the CO_2/C_2H_2 mixture gases, respectively. q_1 and q_2 are CO_2 and C_2H_2 uptake in the gas mixture, respectively, and predicted by the IAST theory. The physical significance of Δq is that it represents the maximum amount of pure C_2H_2 that can be obtained during the adsorption phase of fixed bed separations.

Calculation of Breakthrough Experiments

The calculation method of the C_2H_2 purity is as follows:

$$c = \frac{q_{C_2H_2}}{q_{C_2H_2} + q_{CO_2}}$$

The gas breakthrough gas amount (q_i) (mmol g^{-1}) was calculated by integrating the breakthrough curve $F_i(t)$ as following equation:

$$q_i = \frac{f_i \int_0^{t_1} F_i(t)dt}{22.4 \times m}$$

Where the m represents the adsorbent mass, f_i is the flow rate of gas i (mL min^{-1}); $F_i(t)$ is the function of the breakthrough curve of component i.

Simulation Methodology

Grand canonical Monte Carlo (GCMC) simulations were performed for evaluating the gas adsorption performance. The partial charges of atoms in the framework were originated from the QEq method.[31] The supercell of 3×3×3 was used during the simulation. All the parameters for atoms of **1a** were modeled with the Dreiding forcefield.[32] CO_2 was modeled as a rigid linear triatomic molecule with three charged

LJ interaction sites, for which the LJ potential parameters for O atom (q = -0.35e) and C atom (q = +0.70e) in CO_2 molecule with C-O bond length l = 0.116 nm were taken from the TraPPE force field.[33] The partial charges on the atoms of C_2H_2 molecule was taken from the literature (q_C = -0.266e and q_H = +0.266e), and the LJ potential parameters for C_2H_2 was taken from the Optimized Potentials for Liquid Simulations-All Atom (OPLS-AA) force field.[34] A cutoff distance of 15.4 Å was used for LJ interactions, and the Coulombic interactions were calculated by using Ewald summation. For each run, the 5×10^6 equilibration steps, 5×10^6 production steps were employed.

The binding energy was calculated by DFT method using the Dmol^3 module**.** The calculations were performed under the generalized gradient approximation (GGA) with the Perdew-Burke-Ernzerhof (PBE) exchange-correlation functional and the double numerical plus d-functions (DND) basis set**.** A cutoff of 4.5 Å was used and the SCF convergence was set to 10^{-5}. The binding energy of gas is evaluated by the following equation: $E_{bind} = E_{framework+gas} - E_{framework} - E_{gas}$**,** in which $E_{framework+gas}$ is the total energy of the framework and the adsorbed gas molecule, $E_{framework}$ and E_{gas} are the energies of the framework and gas molecule.

References:

1 W. Yang, A. J. Davies, X. Lin, M. Suyetin, R. Matsuda, A. J. Blake, C. Wilson, W. Lewis, J. E. Parker, C. C. Tang, M. W. George, P. Hubberstey, S. Kitagawa, H. Sakamoto, E. Bichoutskaia, N. R. Champness, S. Yang and M. Schröder, Selective CO_2 uptake and inverse CO_2/C_2H_2 selectivity in a dynamic bifunctional metal-organic framework, *Chem. Sci.*, 2012, **3**, 2993-2999.

2 M. L. Foo, R. Matsuda, Y. Hijikata, R. Krishna, H. Sato, S. Horike, A. Hori, J. Duan, Y. Sato, Y. Kubota, M. Takata and S. Kitagawa, An adsorbate discriminatory gate effect in a flexible porous coordination polymer for selective adsorption of CO_2 over C_2H_2, *J. Am. Chem. Soc.*, 2016, **138**, 3022–3030.

3 K.-J. Chen, H. S. Scott, D. G. Madden, T. Pham, A. Kumar, A. Bajpai, M. Lusi, K. A. Forrest, B. Space, J. J. Perry and M. J. Zaworotko, Benchmark C_2H_2/CO_2 and

CO_2/C_2H_2 separation by two closely related hybrid ultramicroporous materials, *Chem*, 2016, **1**, 753–765.

4 L. Li, J. Wang, Z. Zhang, Q. Yang, Y. Yang, B. Su, Z. Bao and Q. Ren, Inverse adsorption separation of CO_2/C_2H_2 mixture in cyclodextrin-based metal–organic frameworks, *ACS Appl. Mater. Interfaces*, 2019, **11**, 2543–2550.

5 D. Ma, Z. Li, J. Zhu, Y. Zhou, L. Chen, X. Mai, M. Liufu, Y. Wu and Y. Li, Inverse and highly selective separation of CO_2/C_2H_2 on a thulium–organic framework, *J. Mater. Chem. A*, 2020, **8**, 11933-11937.

6 O. T. Qazvini, R. Babarao and S. G. Telfer, Selective capture of carbon dioxide from hydrocarbons using a metal-organic framework, *Nat. Commun.*, 2021, **12**, 197.

7 Y. Xie, H. Cui, H. Wu, R.-B. Lin, W. Zhou and B. Chen, Electrostatically driven selective adsorption of carbon dioxide over acetylene in an ultramicroporous material, *Angew. Chem. Int. Ed.*, 2021, **60**, 9604-9609.

8 Y. Gu, J.-J. Zheng, K. Otake, M. Shivanna, S. Sakaki, H. Yoshino, M. Ohba, S. Kawaguchi, Y. Wang, F. Li and S. Kitagawa, Host–guest interaction modulation in porous coordination polymers for inverse selective CO_2/C_2H_2 separation, *Angew. Chem. Int. Ed.*, 2021, **60**, 11688-11694.

9 Z. Zhang, S. B. Peh, R. Krishna, C. Kang, K. Chai, Y. Wang, D. Shi and D. Zhao, Optimal pore chemistry in an ultramicroporous metal–organic framework for benchmark inverse CO_2/C_2H_2 separation, *Angew. Chem. Int. Ed.*, 2021, **60**, 17198-17204.

10 L.-Z. Cai, Z.-Z. Yao, S.-J. Lin, M.-S. Wang and G.-C. Guo, Photoinduced electron-transfer (PIET) strategy for selective adsorption of CO_2 over C_2H_2 in a MOF, *Angew. Chem. Int. Ed.*, 2021, **60**, 18223-18230.

11 X.-Y. Li, Y. Song, C.-X. Zhang, C.-X. Zhao and C. He, Inverse CO_2/C_2H_2 separation in a pillared-layer framework featuring a chlorine-modified channel by quadrupole-moment sieving, *Sep. Purif. Technol.*, 2021, **279**, 119608.

12 Y. Shi, Y. Xie, H. Cui, Y. Ye, H. Wu, W. Zhou, H. Arman, R.-B. Lin and B. Chen, Highly selective adsorption of carbon dioxide over acetylene in an

ultramicroporous metal–organic framework, *Adv. Mater.*, 2021, **33**, 2105880.

13 H. Cui, Y. Xie, Y. Ye, Y. Shi, B. Liang and B. Chen, An ultramicroporous metal-organic framework with record high selectivity for inverse CO_2/C_2H_2 separation, *B. Chem. Soc. Jpn.*, 2021, **94**, 2698–2701.

14 C. Hao, H. Ren, H. Zhu, Y. Chi, W. Zhao, X. Liu and W. Guo, CO_2-favored metal–organic frameworks SU-101(M) (M = Bi, In, Ga, and Al) with inverse and high selectivity of CO_2 from C_2H_2 and C_2H_4, *Sep. Purif. Technol.*, 2022, **290**, 120804.

15 L.-N. Ma, G.-D. Wang, L. Hou, Z. Zhu and Y.-Y. Wang, Efficient one-step purification of C_1 and C_2 hydrocarbons over CO_2 in a new CO_2-selective MOF with a gate-opening effect, *ACS Appl. Mater. Interfaces*, 2022, **14**, 26858–26865.

16 J. Cui, Z. Qiu, L. Yang, Z. Zhang, X. Cui and H. Xing, Kinetic-sieving of carbon dioxide from acetylene through a novel sulfonic ultramicroporous material, *Angew. Chem. Int. Ed.*, 2022, **134**, e202208756.

17 C. He, P. Zhang, Y. Wang, Y. Zhang, T. Hu, L. Li and J. Li, Thermodynamic and kinetic synergetic separation of CO_2/C_2H_2 in an ultramicroporous metal-organic framework, *Sep. Purif. Technol.*, 2023, **304**, 122318.

18 J. Yu, J. Zhang, P. Zhang, Y. Wang, S.-N. Li and Q.-G. Zhai, Controllable inverse C_2H_2/CO_2 separation in ultra-stable Zn-organic frameworks for efficient removal of trace CO_2 from acetylene, *J. Mater. Chem. A*, 2022, **10**, 23630-23638.

19 H. Zhu, W. Xue, H. Huang, L. Chen, H. Liu and C. Zhong, Water boosted CO_2/C_2H_2 separation in L-arginine functionalized metal-organic framework, *Nano Res.*, 2023, **16**, 6113–6119.

20 C. Hao, Z. Ge, R. Krishna, H. Ren, H. Zhu, Y. Chi, W. Zhao, X. Liu and W. Guo, Fine-tuning channel structure and surface chemistry of stable bismuth-organic frameworks for efficient C_2H_4 purification through reversely trapping CO_2 and C_2H_2, *Chem. Eng. J.*, 2023, **471**, 144533.

21 J. Yang, M. Tong, G. Han, M. Chang, T. Yan, Y. Ying, Q. Yang and D. Liu, Solubility-boosted molecular sieving-based separation for purification of acetylene in core–shell IL@MOF composites, *Adv. Funct. Mater.*, 2023, **33**, 2213743.

22 M. Cavallo, C. Atzori, M. Signorile, F. Costantino, D. M. Venturi, A. Koutsianos,

K. A. Lomachenko, L. Calucci, F. Martini, A. Giovanelli, M. Geppi, V. Crocellà and M. Taddei, Cooperative CO_2 adsorption mechanism in a perfluorinated Ce^{IV}-based metal organic framework, *J. Mater. Chem. A*, 2023, **11**, 5568-5583.

23 Q. Liu, S. G. Cho, J. Hilliard, T.-Y. Wang, S.-C. Chien, L.-C. Lin, A. C. Co and C. R. Wade, Inverse CO_2/C_2H_2 separation with MFU-4 and selectivity reversal via postsynthetic ligand exchange, *Angew. Chem. Int. Ed.*, 2023, **62**, e202218854.

24 W. Wang, G.-D. Wang, B. Zhang, X.-Y. Li, L. Hou, Q.-Y. Yang and B. Liu, Discriminatory gate-opening effect in a flexible metal–organic framework for inverse CO_2/C_2H_2 separation, *Small*, 2023, **19**, 2302975.

25 Z. Zhang, Z. Deng, H. A. Evans, D. Mullangi, C. Kang, S. B. Peh, Y. Wang, C. M. Brown, J. Wang, P. Canepa, A. K. Cheetham and D. Zhao, Exclusive recognition of CO_2 from hydrocarbons by aluminum formate with hydrogen-confined pore cavities, *J. Am. Chem. Soc.*, 2023, **145**, 11643−11649.

26 S. Geng, H. Xu, C.-S. Cao, T. Pham, B. Zhao and Z. Zhang, Bioinspired design of a giant [Mn_{86}] nanocage-based metal-organic framework with specific CO_2 binding pockets for highly selective CO_2 separation, *Angew. Chem. Int. Ed.*, 2023, **62**, e202305390.

27 S.-Q. Yang, R. Krishna, H. Chen, L. Li, L. Zhou, Y.-F. An, F.-Y. Zhang, Q. Zhang, Y.-H. Zhang, W. Li, T.-L. Hu and X.-H. Bu, Immobilization of the polar group into an ultramicroporous metal–organic framework enabling benchmark inverse selective CO_2/C_2H_2 separation with record C_2H_2 production, *J. Am. Chem. Soc.*, 2023, **145**, 13901–13911.

28 Z. Zhang, Y. Chen, K. Chai, C. Kang, S. B. Peh, H. Li, J. Ren, X. Shi, X. Han, C. Dejoie, S. J. Day, S. Yang and D. Zhao, Temperature-dependent rearrangement of gas molecules in ultramicroporous materials for tunable adsorption of CO_2 and C_2H_2, *Nat. Commun.*, 2023, **14**, 3789.

29 Y. Li, X. Wang, H. Zhang, L. He, J. Huang, W. Wei, Z. Yuan, Z. Xiong, H. Chen, S. Xiang, B. Chen and Z. Zhang, A microporous hydrogen bonded organic framework for highly selective separation of carbon dioxide over acetylene, *Angew. Chem. Int. Ed.*, 2023, **62**, e202311419.

30 J.-H. Li, Y.-W. Gan, J.-X. Chen, R.-B. Lin, Y. Yang, H. Wu, W. Zhou, B. Chen and X.-M. Chen, Reverse separation of carbon dioxide and acetylene in two isostructural copper pyridine - carboxylate frameworks, *Angew. Chem. Int. Ed.*, 2024, **63**, e202400823.

31 A. K. Rappé and W. A. Goddard III, Charge equilibration for molecular dynamics simulations, *J. Phys. Chem.*, 1991, **95**, 3358–3363.

32 S. L. Mayo, B. D. Olafson and W. A. Goddard III, DREIDING: a generic force field for molecular simulations, *J. Phys. Chem.*, 1990, **94**, 8897–8909.

33 J. J. Potoff and J. I. Siepmann, Vapor–liquid equilibria of mixtures containing alkanes, carbon dioxide, and nitrogen, *AIChE J.*, 2001, **47**, 1676–1682.

34 W. L. Jorgensen, D. S. Maxwell and J. Tirado-Rives, Development and testing of the OPLS all-atom force field on conformational energetics and properties of organic liquids, *J. Am. Chem. Soc.*, 1996, **118**, 11225–11236.